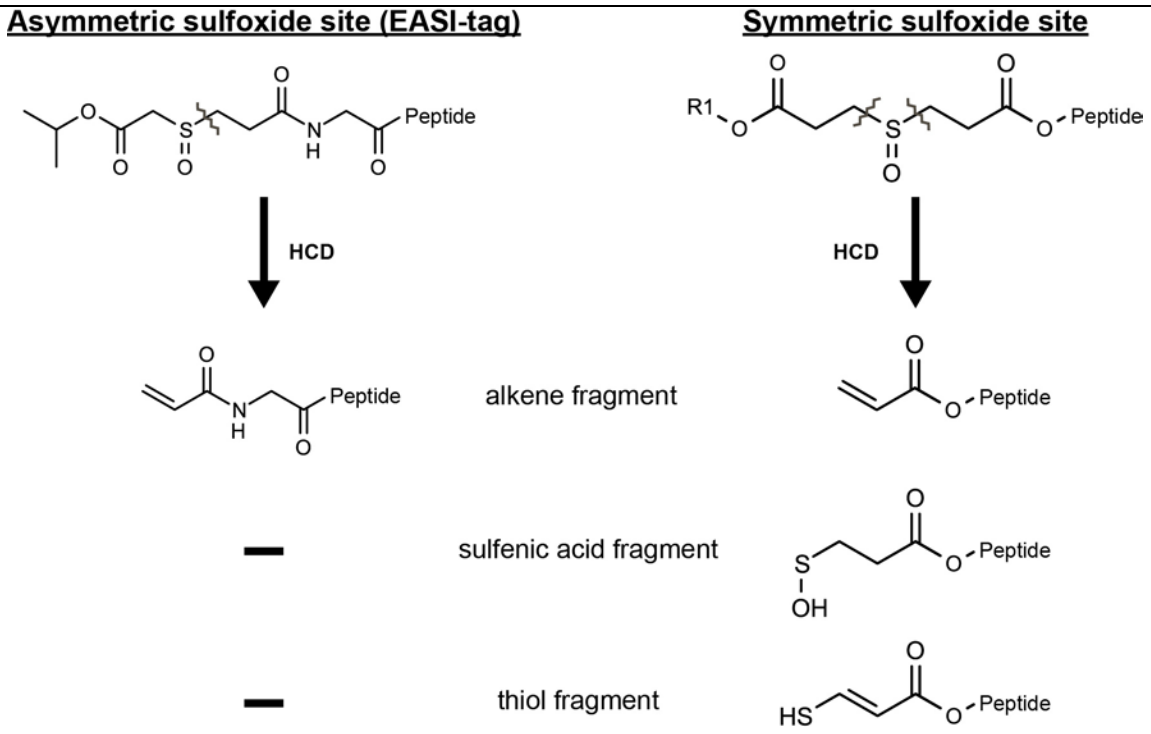

Supplementary Figure 1

Fragmentation of asymmetric and symmetric sulfoxide moieties.

Fragments generated upon HCD-induced cleavage of an asymmetric sulfoxide site as it is present in EASI-tag (left panel) and of a symmetric sulfoxide site as it is present in MS-cleavable crosslinkers (right panel). Here, ‘asymmetry’ refers to the different chemical constitution of the residues on either side of the sulfoxide.

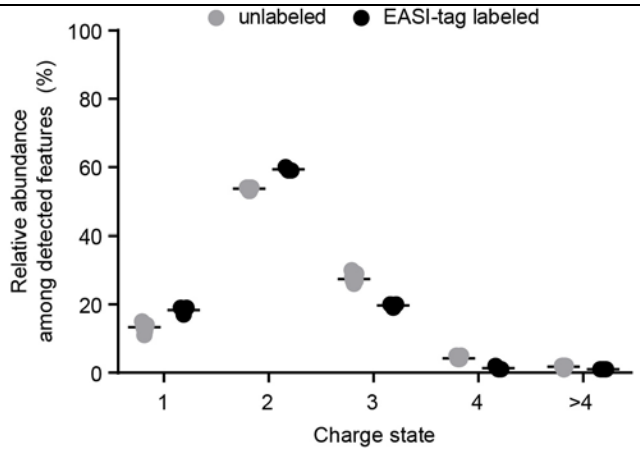

Supplementary Figure 2

Charge state distribution of unlabeled and EASI-tag-labeled peptides.

Distribution of charge states for all features detected by MaxQuant for unlabeled HeLa peptides and EASI-tag-labeled peptides from the one and two proteome experiments for (N=9 for unlabeled and N=3 for EASI-tag-labeled). The center bars indicate the mean values.

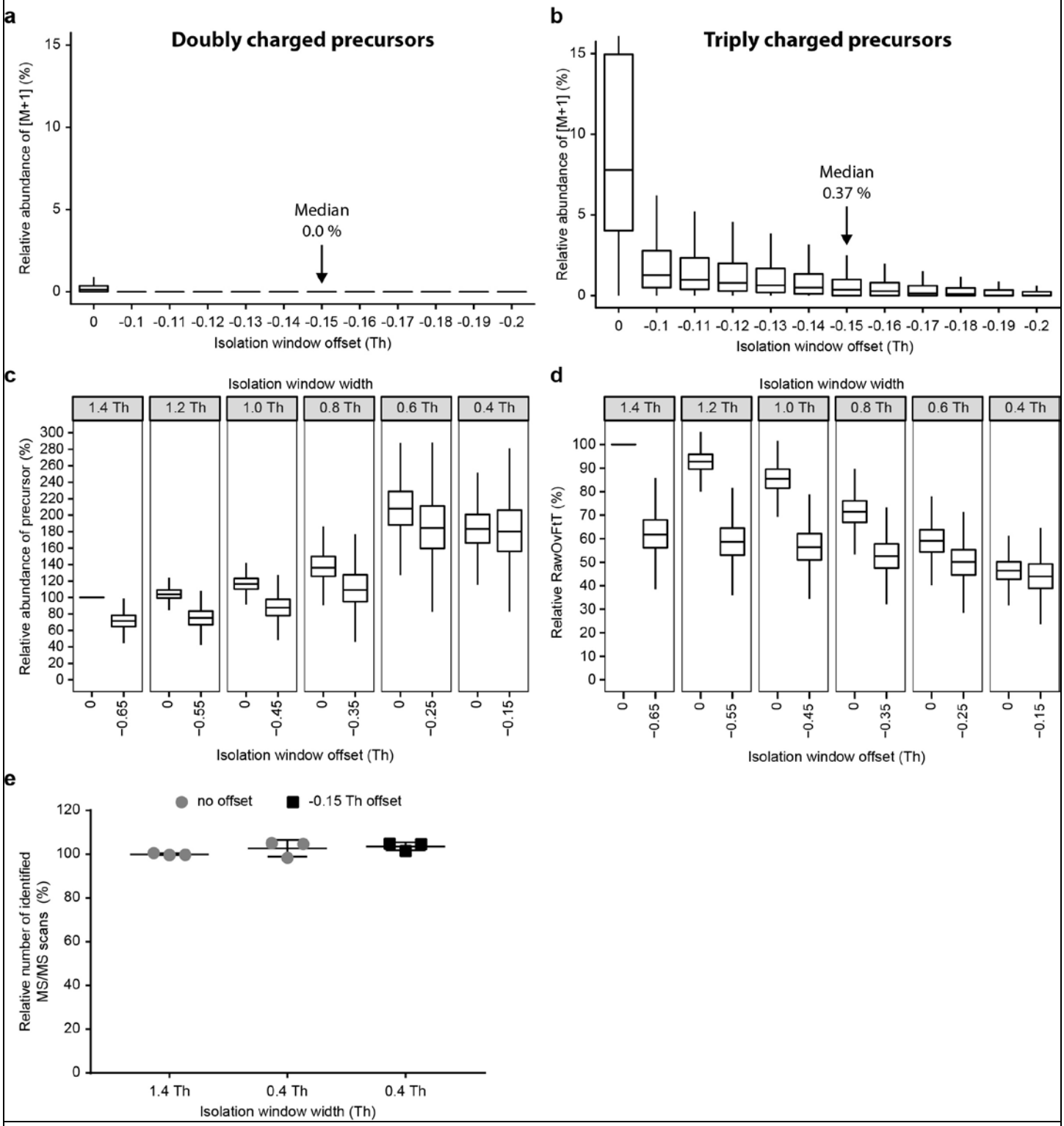

Supplementary Figure 3

Optimization of the asymmetric isolation window by analyses of tryptic HeLa digests.

(a) Abundance of the M+1 isotopic peak in MS/MS scans relative to the monoisotopic precursor ion as a function of the isolation window offset for an isolation width of 0.4 Th and only doubly charged precursor ions (N=4,413) (b) As above but only for triply charged precursor ions (N=2,182). (c) Abundance of the isolated precursor ion in MS/MS scans relative to its abundance when isolated without offset and an 1.4 Th window width (N=5468) (d) RawOvFtT in MS/MS scans relative to the RawOvFtT values with an isolation width of 1.4 Th and without an offset (N=5468) (e) Number of identified MS/MS scans relative to the number of identified MS/MS scans with an 1.4 Th isolation window width and without an offset (N=3). The center bars indicate the mean values an error bars show the standard deviation. Boxplot elements: center line = median, lower and upper box limits = first and third quartiles, whiskers = maximum 1.5x inter-quartile range.

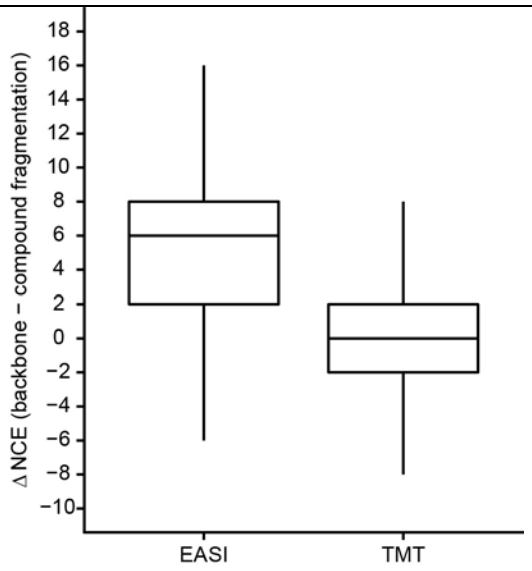

Supplementary Figure 4

Comparison of label fragmentation vs. peptide backbone fragmentation.

(a) EASI- and TMT-labeled HeLa peptides were fragmented with normalized collision energies between 10 and 34. ΔNCE was calculated as the difference of label fragmentation versus peptide backbone fragmentation (N = 10,321 precursors for EASI and 12,875 for TMT). Boxplot elements: center line = median, lower and upper box limits = first and third quartiles, whiskers = maximum 1.5x inter-quartile range.

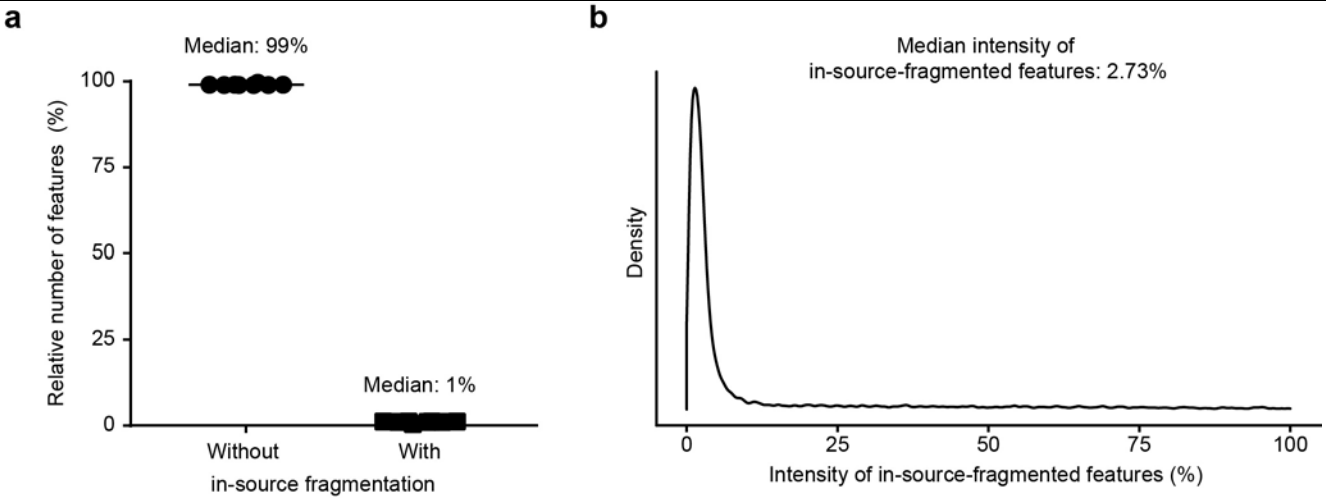

Supplementary Figure 5

Analysis of in-source fragmentation of EASI-tag-labeled HeLa digests.

(a) EASI-tag-zero labeled HeLa peptides were fractioned by high pH reversed-phase and analyzed by LC-MS/MS. The relative number of features with a detectable in-source fragmentation resulting in fragmentation of EASI-tag was determined for each fraction (N=8 raw files and a total of 917,235 features). (b) The intensities of the in-source-fragmented features were determined for each fraction in relation to their unfragmented counterpart (N = 8 raw files and a total of 8,839 features).

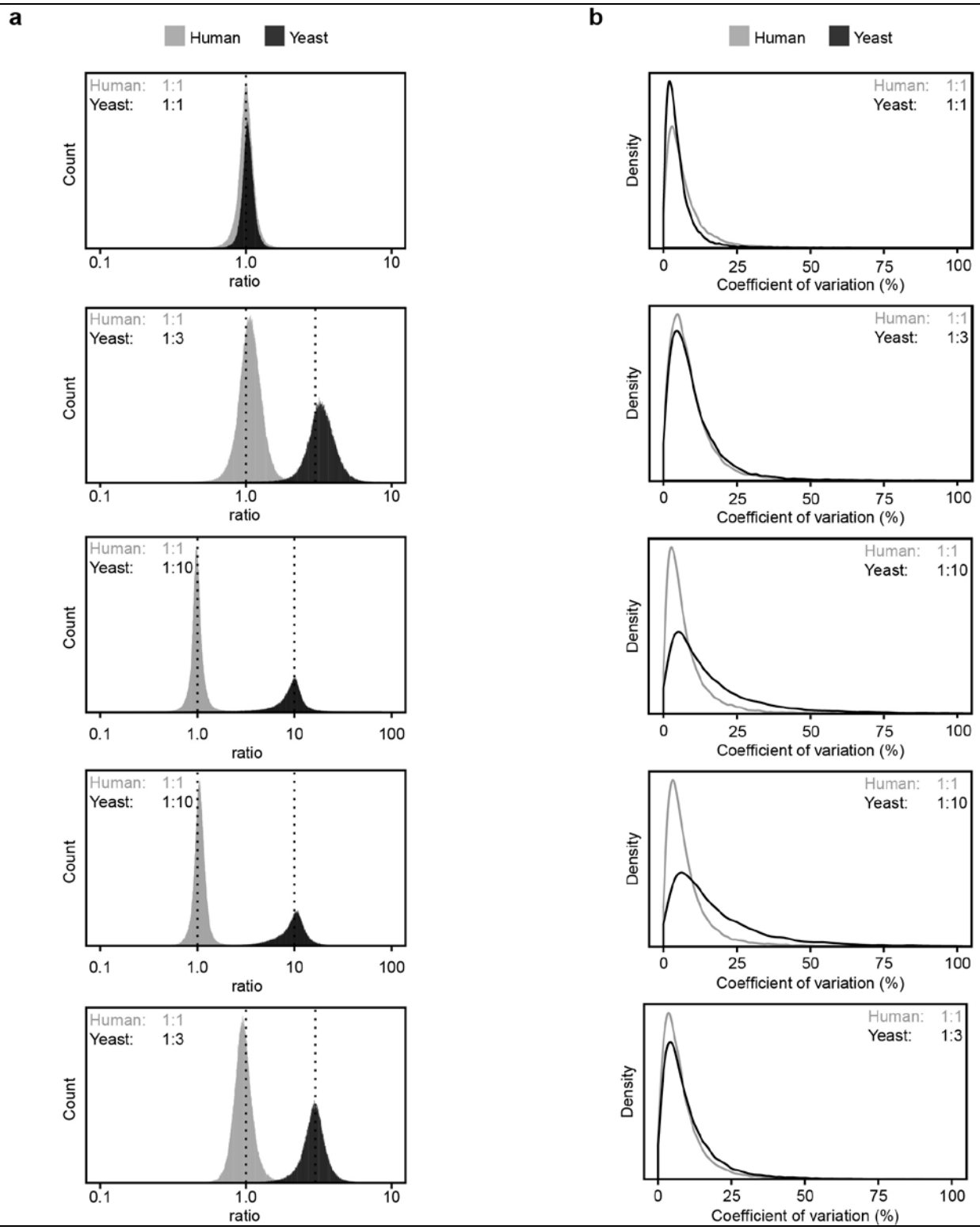

Supplementary Figure 6

Distribution of ratios and coefficients of variation for EASI-tagged peptides.

(a) Distribution of peptide-coupled reporter ion ratios (log10) in MS/MS scans of yeast (mixing ratio 1:3:10:10:3:1) and human (mixing

ratio 1:1:1:1:1:1) peptides (N=369,591, 375,384, 377,496, 377,839 and 378,101 for human channels 0 to 4 and 224,098, 209,244, 146,253, 152,255 and 215,707 for yeast channels 0 to 4). (b) Distribution of the coefficients of variation for EASI-tag quantified yeast and human peptides in three replicate injections (N= 39,400, 39,827, 39,898, 39,930 and 39,882 unique sequences for human channels 0 to 4 and 20,738, 19,947, 15,657, 16,097 and 20,230 unique sequences for yeast channels 0 to 4).